Pulmonary 4D flow CMR imaging in Landrace pigs under rest and stress

Alessandro Faragli
Deutsches Herzzentrum der Charité
Markus Hüllebrand
Deutsches Herzzentrum der Charité
Amy Berendsen
Eindhoven University of Technology
Laia Tirapu Solà
Hospital Moises Broggi
Francesco Paolo Lo Muzio
Deutsches Herzzentrum der Charité
Collin Götze
Deutsches Herzzentrum der Charité
Radu Tanacli
Deutsches Herzzentrum der Charité
Patrick Doeblin
Deutsches Herzzentrum der Charité
Christian Stehning
Philips Healthcare
Bernhard Schnackenburg
Philips Healthcare
Frans Van der Vosse
Eindhoven University of Technology
Eike Nagel
Goethe University Hospital Frankfurt
Heiner Post
Contilia Heart and Vessel Centre, St. Marien-Hospital Mülheim
Anja Hennemuth
Deutsches Herzzentrum der Charité
Alessio Alogna
Deutsches Herzzentrum der Charité

Sebastian Kelle

sebastian.kelle@dhzc-charite.de

Deutsches Herzzentrum der Charité

Research Article

Keywords: Cardiovascular magnetic resonance, 4D flow, pulmonary circulation, flow, velocity, pigs

Posted Date: August 2nd, 2023

DOI: https://doi.org/10.21203/rs.3.rs-3209114/v1

Additional Declarations: Competing interest reported. AH is a member of the management board of Fraunhofer Institute for Digital Medicine MEVIS, Berlin, Germany. The other authors declare that the research was conducted in the absence of any commercial or financial relationships that could be construed as a potential conflict of interest.

Abstract

Introduction:

CMR 4D flow is a promising technique for assessing vessel hemodynamics. However, its current utilization is limited due to the lack of reference values, particularly for pulmonary vessels, generally understudied. With the purpose to serve for future research studies, we have analysed the pulmonary flow and velocity in Landrace pigs at both rest and stress by utilizing the software MEVISFlow.

Methods:

Nine (n=9) healthy Landrace pigs were acutely instrumented closed-chest and transported to the CMR facility for evaluation. After baseline (BL) measurements, dobutamine (Dob) was administrated to achieve a 25% increase in heart rate compared to baseline values. 4D flow images from the pigs during both rest and stress states have been analysed through MEVISFlow software by two independent observers. In detail, we examined peak flow and peak velocity of the pulmonary trunk (PT) and both left and right pulmonary arteries (LPA and RPA, respectively).

Results:

A significant difference between BL and Dob regarding both peak flow and peak velocity in all the pulmonary vessels was observed. Peak flow changed from 0.09 L/min to 0.14 L/min in PT, from 0.04 L/min to 0.07 L/min in LPA and from 0.05 L/min vs 0.07 L/min in RPA. Peak velocity changed from 0.90 m/s to 1.40 m/s in PT, from 0.80 m/s to 1.40 m/s in LPA and from 0.80 m/s to 1.33 m/s in RPA.

Conclusions:

The current study showed that peak flow and peak velocity assessed through pulmonary 4D flow follow the physiological alterations during systole and diastole and after stress induced by dobutamine.

Introduction

Magnetic Resonance Angiography (MRA) is an established technique employed to analyse the vascular system in clinical practice (1). MRA is generally performed to assess the vessels' morphology and investigate anatomical abnormalities following the administration of a contrast agent (2). However, it is a contraindication in patients with severe renal failure and may be associated with allergic reactions, including anaphylactic shock (2, 3). Phase-contrast MRA has emerged as a technique being able to assess both anatomy and the function of the vessels accurately by avoiding the injection of contrast agent (4). Besides anatomy assessment, physiology details are important in making a thorough clinical diagnosis and therefore parameters such as flow amplitude and uniformity, jet velocity and regurgitant fractions are paramount additional features to characterise, stage and follow-up cardiovascular disease. Currently, 2D phase-contrast (PC) is the most used flow-measuring image acquisition sequence utilizing velocity-encoding in a single direction. This allows the user to examine

shunts, regurgitations, and collateral flows (5). Each 2D flow measurement requires a breath-hold, making the use of this technique difficult in several patients with heart diseases of different entities (6), and may impede the consistency of the individually acquired slices.

Recently, 4D flow has emerged as a promising new technique aimed at the assessment of anatomy and flow in a more accurate way than the 2D flow imaging, and without administration of gadolinium contrast agent (7), offering several advantages compared to 2D flow (7, 8). For instance, 4D flow analysis allows measuring velocity in all three spatial directions over time throughout the cardiac cycle (3D + time = 4D) making velocity measurements more accurate (8). The velocity field measured with 4D flow can be used to estimate relative pressure gradients via the Navier-Stokes equation (9). Another advantage of the 4D flow approach is the possibility to derive time-resolved pressure maps in any vessel of interest.

Nonetheless, the main challenges of 4D flow analysis encompass the post-processing of the large data obtained and the necessary corrections performed through a specific software to adjust for gradient field distortions (10). Thus, 4D flow has been mainly utilized for research purposes as the lack of software standardization and consequent reproducibility represent still an unresolved issue (11). On the other side, there is a high need to utilize MRA techniques to develop disease models, and reference values for pre-clinical studies are lacking (12). This is particularly true for large animals, especially regarding pulmonary circulation, which is generally understudied compared to the aorta and arterial vessels (13-15). Indeed, to our knowledge, no studies analysed how flow and velocity in the pulmonary trunk and pulmonary arteries are affected at rest and after dobutamine infusion, even if such stress test is generally performed in the clinics and pre-clinical studies. The objective of the current study was to analyse flow and velocity measured through pulmonary 4D flow under both rest and stress conditions in a cohort of Landrace pigs to provide reference values for future studies.

Methods

Data from n=9 Landrace pigs were selected from an already published study cohort from our group, where dobutamine stress testing was performed (12, 16-18). The experimental protocols were approved by the local bioethics committee of Berlin, Germany (G0138/17) and conform to the "European Convention for the Protection of Vertebrate Animals used for Experimental and other Scientific Purposes" (Council of Europe No 123, Strasbourg 1985).

Experimental protocol and CMR acquisition

Briefly, female Landrace pigs were acutely instrumented, and the animals were transported to the MRI facility for measurements, where the pigs were ventilated with an MRI-compatible machine (Titus, Dräger Medical, Germany). After baseline measurements (BL), dobutamine (Dob) stress was performed. Dobutamine infusion was titrated, aiming at a 25% heart rate increase compared to baseline values. MR imaging was performed on a 3T clinical MR scanner (Ingenia, Philips Healthcare). 4D PC data were acquired with a 3D T1-weighted fast field echo (FFE) sequence with flow encoding gradients in three orthogonal axes (FH, RL, AP), in combination with retrospective gating to the electrocardiograph (ECG)

cycle with 25 heart phases. Data were acquired in sagittal orientation, covering the entire heart and outflow tract. An anterior- and posterior phased array coil was employed for signal reception. Typical scan parameters were as follows: Acquired FOV FH/RL/AP = 180 × 87 × 288 mm^3, acquired resolution = 2.8 × 2.8 × 2.8 mm^3, reconstructed resolution = 1.5 × 1.5 × 2.8mm^3, VENC along all three axes = 250 cm/s, TR/TE/flip = 3.8 ms/2.4 ms/5°, SENSE acceleration factor 2, bandwidth 2500 Hz / pixel. The scan time was on the order of 10 minutes. After the MRI measurements were concluded, the animals were transported back to the operating room for sacrifice.

CMR image analysis

The resulting magnitude image and three velocities encoded images were imported in the software MEVISFlow (Fraunhofer MEVIS, Bremen, Germany) (19). Pre-processing was applied, with noise-masking, antialiasing, automatic correction for eddy currents, and phase unwrapping as provided by MEVISFlow (20). It became apparent that the vector fields were not always imported correctly. A vector field correction was necessary to obtain the correct vector fields, which meant inverting the *x* and *z* axes for almost all scans. Moreover, not all imported scans started at the correct time in the cardiac cycle due to the triggering of the MRI acquisition being half a heartbeat later than the r-wave. This was manually corrected by rearranging the timepoints. Afterward, the pulmonary trunk (PT) and pulmonary arteries were located and segmented manually, which resulted in a mask. Regions of interest (ROI) were placed by manually encircling the vessel of interest at three locations (Figure 1): in the pulmonary trunk, before the vessel starts to dilate, at the left pulmonary artery (LPA) just after the first branch and in the right pulmonary artery (RPA) at the same height as in the LPA. These ROIs were propagated through time over one cardiac cycle.

The hemodynamic parameters obtained were:

- Flow: forward and backward flows

- Regurgitant fraction

- Peak flow

- Peak velocity

- Normalized Flow Displacement (NFD)

NFD is defined as the distance between the center of the flow ($\overrightarrow{cv_j}$) and the center of the vessel ($\overrightarrow{cg_j}$), normalized by the vessel diameter, following the definition by Sigovan et al (21). A value of 0 means the flow is centered, and 1 means the flow is not centered. NFD is described by the following formula:

$NFD_j = \frac{\left|\overrightarrow{cv_j} - \overrightarrow{cg_j}\right|}{D_j}$ where

$\overrightarrow{cv_j} = \frac{\sum_{i=1}^{m_j} \overrightarrow{r_i} \times |\overrightarrow{u_i}|}{\sum_{i=1}^{m_j} |\overrightarrow{u_i}|}$ and $\overrightarrow{cg_j} = \frac{\sum_{i=1}^{m_j} \overrightarrow{r_i}}{m_j}$

- Through Flow Degree (TFD)

TFD is defined as the average ratio of through-plane velocity magnitudes ($\vec{u}_{TP,i}$) and the sums of through-plane ($\vec{u}_{TP,i}$) and in-plane ($\vec{u}_{IP,i}$) velocity magnitude. TFD is a measure of the flow swirl, which, unlike similar parameters like helicity, incorporates vessel orientation (21). TFD is described by the following formula:

$TFD_j = \frac{1}{m_j} \sum_{i=1}^{m_j} \frac{|\vec{u}_{TP,i}|}{\sqrt{|\vec{u}_{TP,i}|^2 + |\vec{u}_{IP,i}|^2}}$ where

$\vec{u}_{TP,i} = (\overrightarrow{u_i} \times \overrightarrow{n_j})\overrightarrow{n_j}$ and $\vec{u}_{IP,i} = \overrightarrow{u_i} - \vec{u}_{TP,i}$

For evaluation of laminarity, minor flows superimposed to the main predicted flow pattern are evaluated. 0 means there is no in-plane motion (no turbulence).

The angle measured in degrees was defined as the flow angulation in relation to the plane defined by the ROI area.

Statistical analysis

Data were analysed using Microsoft Excel and IBM SPSS Statistics version 23.0 software (SPSS Inc., Chicago, IL, USA) for Windows. Figures were made with GraphPad Prism version 8. All data are presented as mean ± SD. The Shapiro–Wilk test was used to determine whether the data were normally distributed. Data between groups at different inotropic states were analysed by one-way ANOVA for repeated measurements. Post-hoc testing was performed by Tukey's test. Nonparametric variables were compared using the Wilcoxon test. A p-value of < 0.05 was considered statistically significant.

Reproducibility testing

Inter- and intra-observer reproducibility was quantified using intra-class correlation coefficient (ICC). Agreement was considered excellent for ICC >0.74, good for ICC 0.60–0.74, fair for ICC 0.40–0.59, and poor for ICC <0.40. Data analysis was repeated after four weeks to assess intra-observer agreement. All the operators took the measurements twice, and the average values were taken.

Results

The study population included n=9 Landrace pigs who underwent 4D flow MRI during rest and dobutamine-induced stress conditions. Pulmonary hemodynamic parameters measured at baseline (BL) and during dobutamine (Dob) stress test assessed in PT, LPA, and RPA are reported in Table 1. The anatomical reconstruction of the main pulmonary vessels with their ROIs are shown in Figure 1. Moreover, a previously unreported secondary branch was observed arising from the beginning of the left pulmonary artery, straight after the bifurcation of the pulmonary trunk of every pig (Figure 1).

Pulmonary 4D flow reference values in pigs at baseline and during dobutamine

Through MEVISFlow software, it has been possible to obtain a color-coded graphical reconstruction of the respective increase and decrease of flow and velocity during systole and diastole in the PT, LPA, and RPA at both BL (Figure 2A, 2B) and Dob (Figure 2C, 2D). Then, we then represented the parameters relevant for clinical translation, namely, peak flow and peak velocity obtained from PT, LPA and RPA during both BL and Dob. A significant difference in peak flow and peak velocity has been observed for all the observed pulmonary vessels between rest and stress (Figure 3A, 3C). To highlight the sensitivity of the measurement, we calculated the relative percentage of change for both flow and velocity in PT (Figure 3B and 3D) which was more than 50% between rest and stress. Eventually, through MEVISFlow, a graphical 3D anatomical reconstruction has been obtained, analysing the flow and velocity for the whole pulmonary arterial tree at rest (Figure 4A) and during dobutamine stress (Figure 4B). A video of the flow reconstruction during baseline and dobutamine is presented in the Online Supplements.

Inter and intra-observer variability

All studies were completed, and image quality was sufficient to perform the 4D flow analysis. We performed a reproducibility analysis to detect the level of agreement between observers for the measurements performed in the PT during BL. Parameters obtained by two independent investigators, mean differences ± SD, limits of agreement, and ICC for flow and velocity parameters are presented in Table 2. We observed an excellent intra-observer and inter-observer reproducibility for both parameters during BL. We then performed a Bland-Altman Analysis of the intra- and inter- observer reproducibility analysis of Flow and Velocity in the pulmonary trunk during baseline (see Online Supplements, Figure 1S).

Discussion

Although the accuracy of 4D flow measurements compared to echocardiography has already been proven (15) and validation studies against standard 2D flow CMR have already been performed in humans (22), others have described its parameters to underestimate peak flow rates, making further studies necessary (23, 24). Moreover, few studies have investigated in large animal models the role of flow and velocity in the pulmonary arteries, mostly focusing, instead, on the aorta and arterial vasculature (13, 14).

Regarding animal studies, a recent study by the group of Stam et al. compared invasively measured aorta flow with 2D phase-contrast flow and 4D flow measurements in a cohort of Landrace pigs (13). Flow measurements were performed on 4D flow images at the aortic valve level, in the ascending aorta, and the main pulmonary artery (13). Although the authors showed a strong correlation between invasively measured hemodynamics and both 4D and 2D flow CMR, the assessment of the pulmonary vasculature was not the main purpose of the study and was not thoroughly investigated (13). The study that mostly investigated the pulmonary vasculature in a population of large animals has been performed by the group of Roldan et al. in which they validated 4D flow determined pulmonary vascular resistance against invasive measurements in a canine cohort of acutely induced pulmonary hypertension (25). The study concentrated on demonstrating the feasibility of 4D flow in estimating pulmonary vascular resistance while assessing ventricular function and pulmonary artery hemodynamics in free breathing. However, the study did not provide reference values for pulse wave velocities (25).

Our study showed that both peak flow and peak velocity assessed in the pulmonary arteries through 4D flow finely follow the physiological alterations given by systole and diastole.

Moreover, by dobutamine-induced stress, which caused a heart rate increase of 25% from baseline, we were able to observe a significant increase in both peak flow and peak velocity compared to baseline. Therefore, the observed relative increase of at least 50% for both peak flow and peak velocity between baseline and stress was expected.

We did not observe significant difference in the other hemodynamic parameters measured. In detail, we analysed both NFD and TFD, as parameters of flow displacement. While some studies identified an association between increased NFD and aortic dilation (26-28) and others found it to be related to left ventricular remodelling (29), we did not observe any significant changes as expected because our animal cohort was a healthy one. We found only a significant change in TFD after induction of stress in the RPA, however, we cannot draw any pathophysiological conclusions.

While reproducibility analysis is a standard operating procedure in clinical studies, this is not always the case in pre-clinical ones, where newly developed techniques and methodologies need strong precision and accuracy assessment. On this topic, in a previous study from our group we were able to show a high reproducibility of LV strain measured with CMR-FT (12). In the present study, an excellent reproducibility was observed in the baseline measurements for both peak flow and peak velocity, showing that MEVISFlow may be a software of choice for pulmonary vessels.

The concept behind the present work is to offer reference values of healthy animals for future works, especially in large animal models where there is a need to keep the number of experiments at the minimum. This pilot study may be useful for the realization of future animal models of disease, concerning the pulmonary and right ventricle disease which remain relatively understudied. Interestingly, we underline the discovery of an unreported proximal right pulmonary artery branch in two of the Landrace pigs drawing the attention to the chances that 4D flow may offer to animal research.

Nevertheless, our study is not exempted from limitations that need to be addressed. The experiments were performed during anaesthesia, being a possible confounder for reproducibility of the measurements. The study is limited due to the small number of animals, and larger sample size may be required to detect more subtle differences. The addition of a 25% dropout rate (proportion of eligible subjects who will not complete the study or provide only partial information) before planning a study can further increase the final sample size and confirm the present results. A future analysis should be performed to assess the reproducibility of the 4D flow parameters during stress conditions considering this was not the purpose of the present study.

Conclusions

The current study showed that peak flow and peak velocity assessed through the pulmonary 4D flow method follow the physiological alterations during systole and diastole and after stress induced by dobutamine. In addition, MEVISFlow is a feasible software for measuring pulmonary parameters in a cohort of Landrace pigs under rest and stress and may be further investigated in pre-clinical and clinical studies.

Abbreviations

BL	baseline
CMR	cardiovascular magnetic resonance
Dob	dobutamine
ECG	electrocardiograph
FFE	fast field echo
FT	feature tracking
HR	heart rate
ICC	intraclass correlation coefficient
LPA	left pulmonary artery

MRA	magnetic resonance angiography
MRI	magnetic resonance imaging
NFD	normalized flow displacement
PC	phase contrast
PH	pulmonary hypertension
PT	pulmonary trunk
ROI	region of interest
RPA	right pulmonary artery
SD	standard deviation
TFD	through flow degree

Declarations

Authors' contribution

SK, AA, HP, AF, AJB, AH, FNVV: conceptualization. AF, AA, AJB, LTS, CS: conduction of the experiments, data collection and curation. AF, MH, AJB, LTS, MH: data processing. AJB, MH, CS: methodology. AF, MH, AJB, FPLM, AA, RT, CG, SK: writing-original draft. All: writing-review and editing. All authors contributed to the article and approved the submitted version.

Conflicts of interest

AH is a member of the management board of Fraunhofer Institute for Digital Medicine MEVIS, Berlin, Germany. The other authors declare that the research was conducted in the absence of any commercial or financial relationships that could be construed as a potential conflict of interest.

Acknowledgements of grant support

Alessandro Faragli, Heiner Post, Alessio Alogna and Sebastian Kelle received funding from DZHK (German Centre for Cardiovascular Research—Grant Number: 81X2100305). Sebastian Kelle was supported by a research grant from Philips Healthcare. This work was partially funded by the Deutsche Forschungsgemeinschaft (DFG, German Research Foundation) - SFB-1470 - B06.

References

1. Price RR, Creasy JL, Lorenz CH, Partain CL (1992) Magnetic resonance angiography techniques. Invest Radiol 27(Suppl 2):S27–32
2. Frydrychowicz A, Bley TA, Zadeh ZA, Harloff A, Winterer JT, Hennig J et al (2008) Image analysis in time-resolved large field of view 3D MR-angiography at 3T. J Magn Reson imaging: JMRI 28(5):1116–1124
3. Lin SP, Brown JJ (2007) MR contrast agents: physical and pharmacologic basics. J Magn Reson imaging: JMRI 25(5):884–899
4. Markl M, Harloff A, Bley TA, Zaitsev M, Jung B, Weigang E et al (2007) Time-resolved 3D MR velocity mapping at 3T: improved navigator-gated assessment of vascular anatomy and blood flow. J Magn Reson imaging: JMRI 25(4):824–831
5. Chai P, Mohiaddin R (2005) How we perform cardiovascular magnetic resonance flow assessment using phase-contrast velocity mapping. J Cardiovasc Magn resonance: official J Soc Cardiovasc Magn Reson 7(4):705–716
6. Srichai MB, Lim RP, Wong S, Lee VS (2009) Cardiovascular applications of phase-contrast MRI. AJR Am J Roentgenol 192(3):662–675
7. Dyverfeldt P, Bissell M, Barker AJ, Bolger AF, Carlhall CJ, Ebbers T et al (2015) 4D flow cardiovascular magnetic resonance consensus statement. J Cardiovasc Magn resonance: official J Soc Cardiovasc Magn Reson 17:72
8. Markl M, Chan FP, Alley MT, Wedding KL, Draney MT, Elkins CJ et al (2003) Time-resolved three-dimensional phase-contrast MRI. J Magn Reson imaging: JMRI 17(4):499–506
9. Lorenz R, Bock J, Barker AJ, von Knobelsdorff-Brenkenhoff F, Wallis W, Korvink JG et al (2014) 4D flow magnetic resonance imaging in bicuspid aortic valve disease demonstrates altered distribution of aortic blood flow helicity. Magn Reson Med 71(4):1542–1553
10. Hsiao A, Alley MT, Massaband P, Herfkens RJ, Chan FP, Vasanawala SS (2011) Improved cardiovascular flow quantification with time-resolved volumetric phase-contrast MRI. Pediatr Radiol 41(6):711–720
11. Oechtering TH, Nowak A, Sieren MM, Stroth AM, Kirschke N, Wegner F et al (2023) Repeatability and reproducibility of various 4D Flow MRI postprocessing software programs in a multi-software and multi-vendor cross-over comparison study. J Cardiovasc Magn Reson 25(1):22
12. Faragli A, Tanacli R, Kolp C, Lapinskas T, Stehning C, Schnackenburg B et al (2020) Cardiovascular magnetic resonance feature tracking in pigs: a reproducibility and sample size calculation study. Int J Cardiovasc Imaging 36(4):703–712
13. Stam K, Chelu RG, van der Velde N, van Duin R, Wielopolski P, Nieman K et al (2019) Validation of 4D flow CMR against simultaneous invasive hemodynamic measurements: a swine study. Int J Cardiovasc Imaging 35(6):1111–1118
14. Wentland AL, Wieben O, Shanmuganayagam D, Krueger CG, Meudt JJ, Consigny D et al (2015) Measurements of wall shear stress and aortic pulse wave velocity in swine with familial hypercholesterolemia. J Magn Reson Imaging 41(5):1475–1485

15. Chelu RG, van den Bosch AE, van Kranenburg M, Hsiao A, van den Hoven AT, Ouhlous M et al (2016) Qualitative grading of aortic regurgitation: a pilot study comparing CMR 4D flow and echocardiography. Int J Cardiovasc Imaging 32(2):301–307
16. Faragli A, Tanacli R, Kolp C, Abawi D, Lapinskas T, Stehning C et al (2020) Cardiovascular magnetic resonance-derived left ventricular mechanics-strain, cardiac power and end-systolic elastance under various inotropic states in swine. J Cardiovasc Magn resonance: official J Soc Cardiovasc Magn Reson 22(1):79
17. Faragli A, Alogna A, Lee CB, Zhu M, Ghorbani N, Lo Muzio FP et al (2021) Non-invasive CMR-Based Quantification of Myocardial Power and Efficiency Under Stress and Ischemic Conditions in Landrace Pigs. Front Cardiovasc Med 8:689255
18. Alogna A, Faragli A, Kolp C, Doeblin P, Tanacli R, Confortola G et al (2023) Blood-Oxygen-Level Dependent (BOLD) T2-Mapping Reflects Invasively Measured Central Venous Oxygen Saturation in Cardiovascular Patients. JACC Cardiovasc imaging 16(2):251–253
19. Hennemuth A, Friman O, Schumann C, Bock J, Drexl J, Huellebrand M et al (2011) Fast interactive exploration of 4D MRI flow data. 7964(1):79640E–E
20. Lankhaar J-W, Hofman MBM, Marcus JT, Zwanenburg JJM, Faes TJC, Vonk-Noordegraaf A (2005) Correction of phase offset errors in main pulmonary artery flow quantification. J Magn Reson Imaging 22(1):73–79
21. Sigovan M, Hope MD, Dyverfeldt P, Saloner D (2011) Comparison of four-dimensional flow parameters for quantification of flow eccentricity in the ascending aorta. J Magn Reson Imaging 34(5):1226–1230
22. Chelu RG, Wanambiro KW, Hsiao A, Swart LE, Voogd T, van den Hoven AT et al (2016) Cloud-processed 4D CMR flow imaging for pulmonary flow quantification. Eur J Radiol 85(10):1849–1856
23. Carlsson M, Toger J, Kanski M, Bloch KM, Stahlberg F, Heiberg E et al (2011) Quantification and visualization of cardiovascular 4D velocity mapping accelerated with parallel imaging or k-t BLAST: head to head comparison and validation at 1.5 T and 3 T. J Cardiovasc Magn resonance: official J Soc Cardiovasc Magn Reson 13:55
24. Hanneman K, Sivagnanam M, Nguyen ET, Wald R, Greiser A, Crean AM et al (2014) Magnetic resonance assessment of pulmonary (QP) to systemic (QS) flows using 4D phase-contrast imaging: pilot study comparison with standard through-plane 2D phase-contrast imaging. Acad Radiol 21(8):1002–1008
25. Roldán-Alzate A, Frydrychowicz A, Johnson KM, Kellihan H, Chesler NC, Wieben O et al (2014) Non-invasive assessment of cardiac function and pulmonary vascular resistance in an canine model of acute thromboembolic pulmonary hypertension using 4D flow cardiovascular magnetic resonance. J Cardiovasc Magn resonance: official J Soc Cardiovasc Magn Reson 16(1):23
26. Hope MD, Sigovan M, Wrenn SJ, Saloner D, Dyverfeldt P (2014) MRI hemodynamic markers of progressive bicuspid aortic valve-related aortic disease. J Magn Reson Imaging 40(1):140–145

27. Garcia J, Barker AJ, Murphy I, Jarvis K, Schnell S, Collins JD et al (2015) Four-dimensional flow magnetic resonance imaging-based characterization of aortic morphometry and haemodynamics: impact of age, aortic diameter, and valve morphology. Eur Heart J - Cardiovasc Imaging 17(8):877–884
28. Burris NS, Sigovan M, Knauer HA, Tseng EE, Saloner D, Hope MD (2014) Systolic flow displacement correlates with future ascending aortic growth in patients with bicuspid aortic valves undergoing magnetic resonance surveillance. Invest Radiol 49(10):635–639
29. von Knobelsdorff-Brenkenhoff F, Karunaharamoorthy A, Trauzeddel RF, Barker AJ, Blaszczyk E, Markl M et al (2016) Evaluation of Aortic Blood Flow and Wall Shear Stress in Aortic Stenosis and Its Association With Left Ventricular Remodeling. Circulation: Cardiovascular Imaging. ;9(3):e004038

Tables

Table 1. Measured hemodynamic parameters during rest and stress states. The hemodynamic parameters measured during rest and stress from the pulmonary trunk (PT), the left pulmonary artery (LPA), and the right pulmonary artery (RPA) are displayed (n=9). Data are presented as mean ± SD. A p-value of <0.05 was considered significant. Reg Fraction = regurgitation fraction; NFD = normalized flow displacement; TFD = through flow degree

		Rest		Stress		
		Mean	SD	Mean	SD	p-value
PT	Peak Flow [L/min]	0.09	0.06	0.14	0.05	0.02
	Reg Fraction [%]	0.58	0.91	0.18	0.51	0.33
	Peak Velocity [m/s]	0.90	0.24	1.40	0.21	<0.001
	NFD Mean	0.08	0.02	0.09	0.02	0.42
	TFD Mean	0.56	0.16	0.59	0.14	0.95
	Angle Mean	29.98	23.96	27.06	22.40	0.37
LPA	Peak Flow [L/min]	0.04	0.02	0.07	0.03	0.01
	Reg Fraction [%]	3.47	6.54	2.94	4.63	0.75
	Peak Velocity [m/s]	0.80	0.21	1.40	0.24	<0.001
	NFD Mean	0.08	0.02	0.08	0.02	0.25
	TFD Mean	0.56	0.14	0.58	0.09	0.95
	Angle Mean	36.52	26.02	38.78	20.15	0.76
RPA	Peak Flow [L/min]	0.05	0.03	0.07	0.02	0.02
	Reg Fraction [%]	0.31	0.51	0.24	0.73	0.59
	Peak Velocity [m/s]	0.80	0.21	1.33	0.28	<0.001
	NFD Mean	0.07	0.02	0.07	0.01	0.32
	TFD Mean	0.65	0.06	0.62	0.05	0.02
	Angle Mean	16.20	6.66	22.26	9.76	0.01

Table 2. Inter-observer and intra-observer reproducibility for peak flow and peak velocity during baseline measurement in the PT. An excellent ICC was observed for both intra-observer and inter-observer variability. Results are reported as mean ± SD. CI = confidence interval; ICC = intra-class correlation coefficient; PT = pulmonary trunk; SD = standard deviation

	Parameters	Mean difference ± SD	Limits of Agreement	ICC (95% CI)
Intra-observer variability	**Peak Flow**	-0.01 ± 0.01	-0.01 to 0.01	0.99 (0.99 – 1.00)
	Peak Velocity	-0.02 ± 0.07	-0.11 to 0.15	0.97 (0.90 – 0.99)
Inter-observer variability	**Peak Flow**	-0.01 ± 0.03	-0.06 to 0.05	0.91 (0.62 – 0.98)
	Peak Velocity	-0.03 ± 0.10	-0.24 to 0.16	0.96 (0.82 – 0.99)

Figures

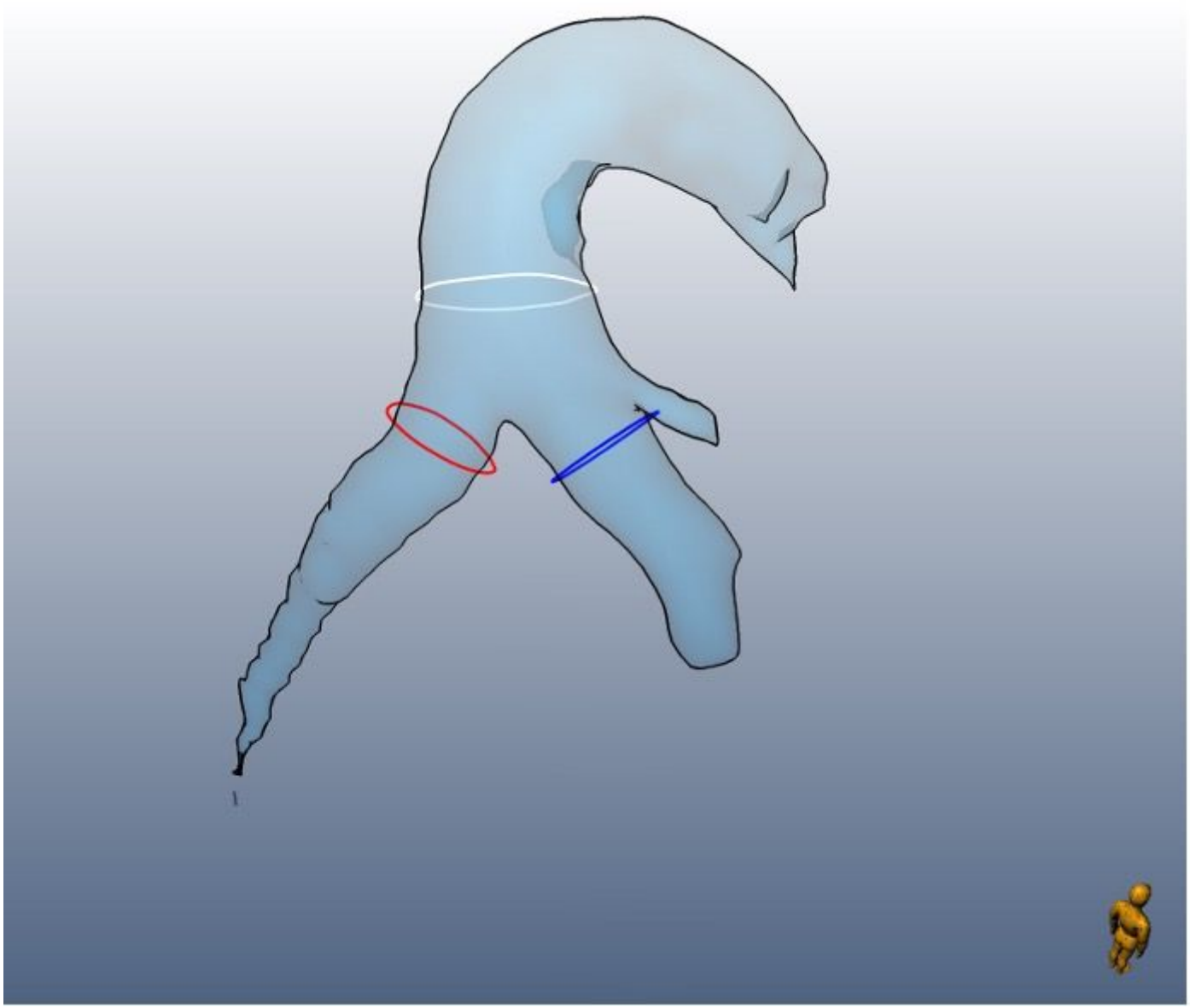

Figure 1

Placement of ROIs in pulmonary arteries in a selected pig.

Represented in white is the main pulmonary trunk (PT), in blue the left pulmonary artery (LPA), while in red the right pulmonary artery (RPA). A previously unreported proximal right branch of the RPA has been detected in two of the animals observed.

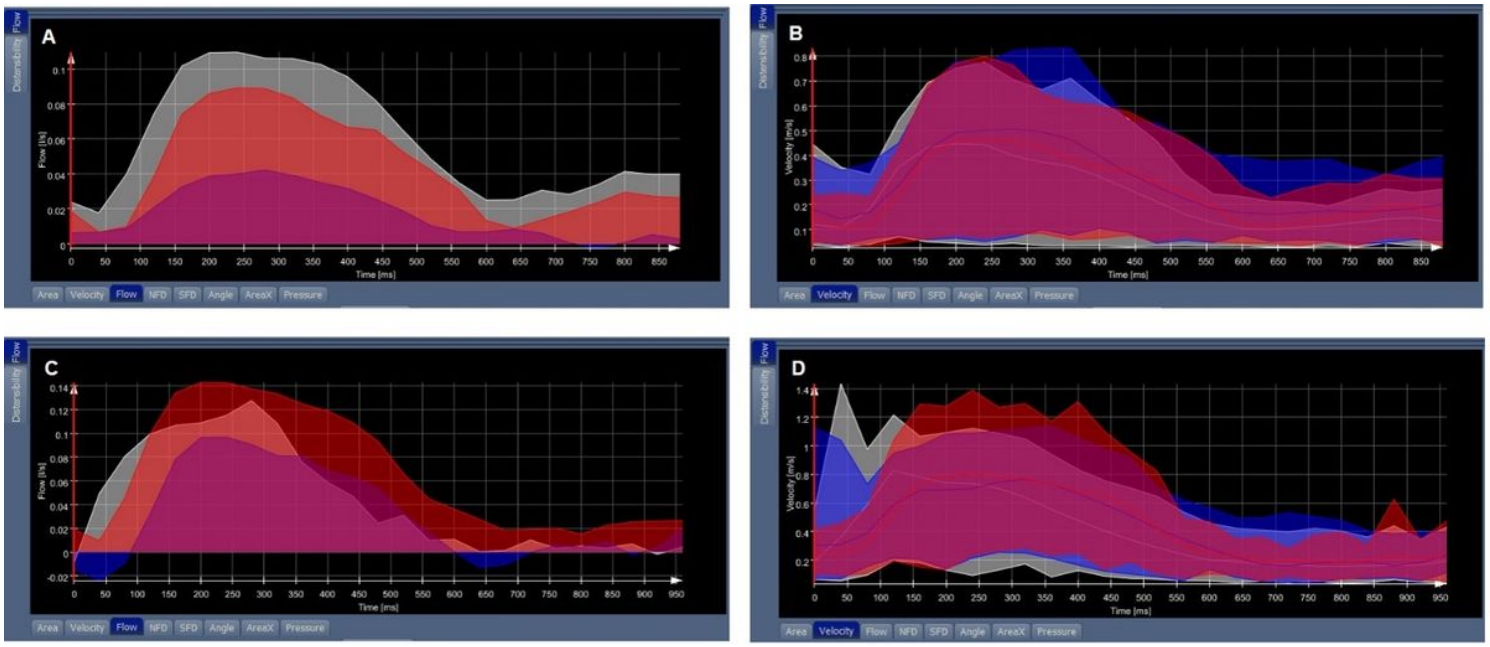

Figure 2

Graphical representation of flow and velocity in one pig during a complete myocardial cycle at baseline. Baseline flow (A) and velocity (B) graphs of pulmonary trunk (grey), left pulmonary artery (blue) and right pulmonary artery (red) are displayed in MEVISFlow during systole and diastole during baseline. We then repeated the same analysis for velocity (C) and flow (D) during dobutamine infusion. As expected, peak flow and peak velocity increase during systole and decrease during diastole. This effect is exacerbated during dobutamine stress.

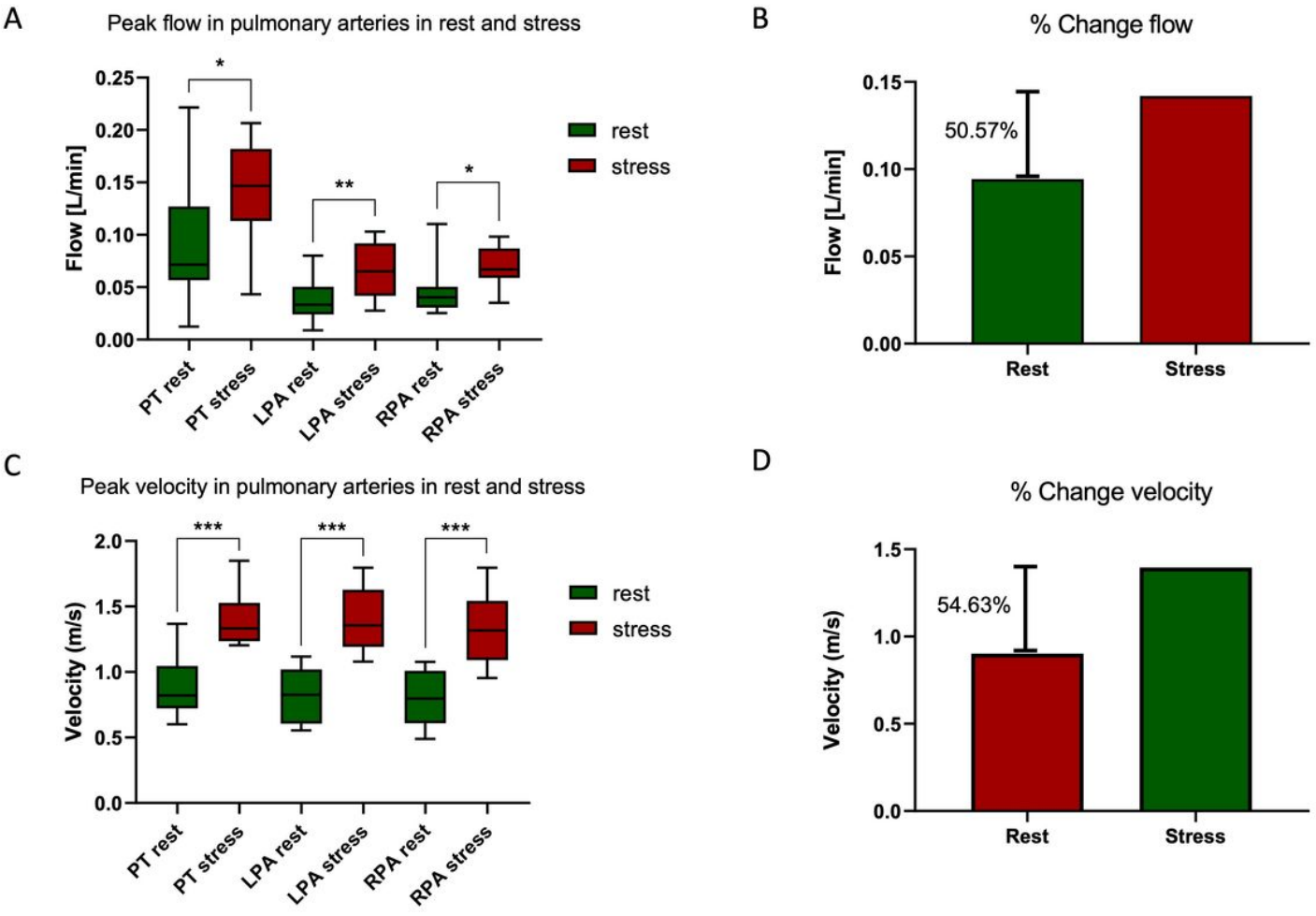

Figure 3

Comparison of peak flow and peak velocity at rest versus stress states. (A) Peak flows in the pulmonary arteries are plotted during rest and stress (box plot 5-95 percentile). (B) Peak flow percentage of change in the PT is displayed between calculated averages at rest and stress. (C) Peak velocities in the pulmonary arteries are plotted in rest and stress (box plot 5-95 percentile). (D) Peak velocity percentage of change in the PT is shown between calculated averages at rest and stress. PT = pulmonary trunk; LPA = left pulmonary artery; RPA = right pulmonary artery

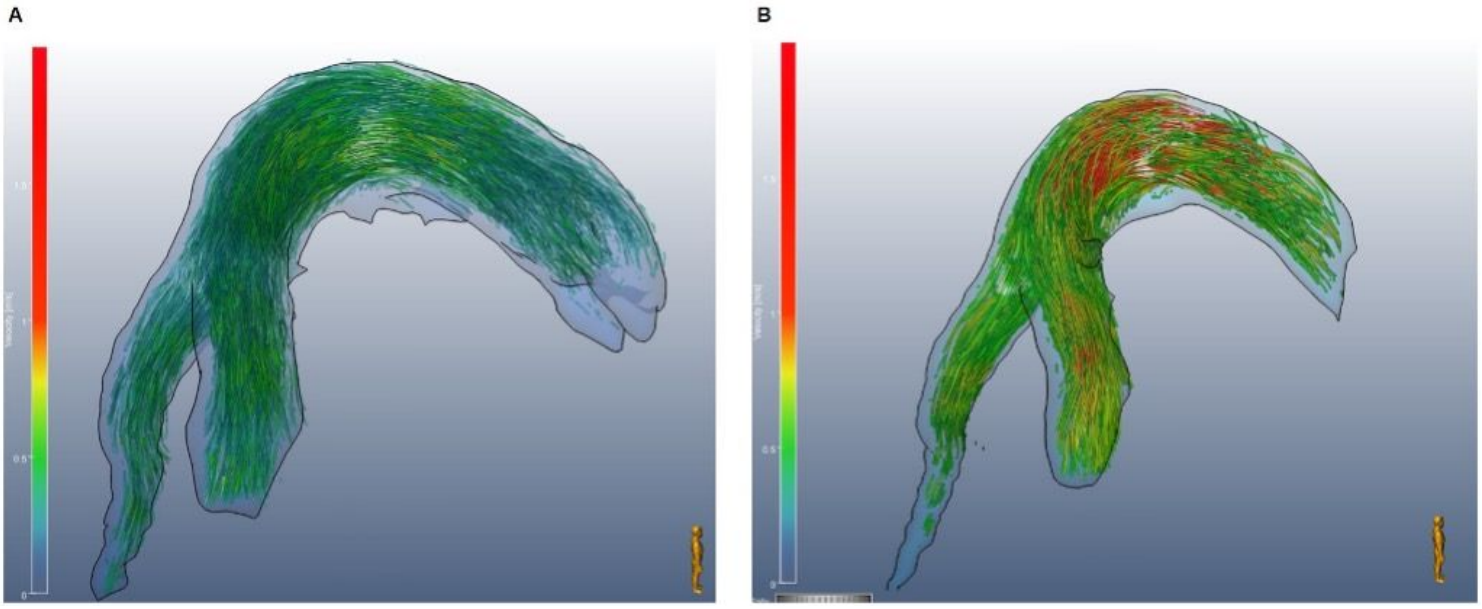

Figure 4

Graphical 3D reconstruction through MEVISFlow at baseline versus dobutamine. (A) Graphical reconstruction of velocity and flow in MEVISFlow during baseline and (B) after stress induced by dobutamine. The scale on the left represents velocity where red is the highest velocity compared to blue representing the lowest.

Supplementary Files

This is a list of supplementary files associated with this preprint. Click to download.

- DobuParticles1.mp4
- BaselineParticles2.mp4
- Figure1S.jpg
- OnlineSupplements.docx